Biophysical Chemistry 18 (1983) 323–337
Elsevier

BPC 00811

ION-SPECIFIC DIFFUSION RATES THROUGH TRANSMEMBRANE PROTEIN CHANNELS

A MOLECULAR DYNAMICS STUDY

Walter FISCHER and Jürgen BRICKMANN

Institut für Physikalische Chemie, Technische Hochschule Darmstadt, Petersenstrasse 20, D-6100 Darmstadt, F.R.G.

Received 16th February 1983
Accepted 30th May 1983

Key words: Ion diffusion; Molecular dynamics simulation; Transmembrane channel; Ion specificity

The migration of different alkali metal cations through a transmembrane model channel is simulated by means of the molecular dynamics technique. The parameters of the model are chosen in close relation to the gramicidin A channel. Coulomb- and van der Waals-type potentials between the ions and flexible carbonyl groups of the pore-forming molecule are used to describe the ion channel interaction. The diffusion properties of the ions are obtained from three-dimensional trajectory calculations. The diffusion rates for the different ions Li^+, Na^+, K^+ and Rb^+ are affected not only by the mass of the particles but also very strongly by their size. The latter effect is more pronounced for rigid channels, i.e., for binding vibrational frequencies of the CO groups with $\tilde{\nu} > 400\ cm^{-1}$. In this range the selectivity sequence for the diffusion rates is the inverse of that expected from normal rate theory but agrees with that found in experiments for gramicidin A.

1. Introduction

Ion transport through biological membranes often takes place via built-in proteins which provide energetically favourable pathways through the non-polar interior of the membrane. These special pathways function either as 'carriers' or as 'pores' [1,2]. In the case of carrier transport, large protein rearrangements in the membrane are responsible for the ionic flow; while for channel diffusion, only small conformational changes of the transport protein are expected. In both cases, the overall transport rate of cations through membranes is affected by three different contributions: association (partly dehydration) of the ion with the membrane, transport from one side to the other (translocation) and dissociation (hydration) of the ion from the membrane into the liquid [3–5]. The aim of the present work is to investigate the microscopic steps of the motion (translocation) along the interior of the channel. We will restrict our considerations to very narrow channels. For these the hydrophilic pathway runs through an array of co-ordination sites produced by polar ligands approximately lining the central hole of the pore. A theoretically and experimentally well studied example of such a system is the cation-permeable gramicidin A channel [6–18]. This polypeptide consists, according to the model of Urry [19,20], of a helix with 6.3 amino acids per turn. The central hole is lined with polar carbonyl groups and has a diameter of about 0.4 nm. The gramicidin A molecule has a known, relatively simple structure, and, therefore transport properties which can be obviously related to structural features. Furthermore, its ideal cationic selectivity and its intercationic specificity make it comparable to many other channels in biological membranes.

In a variety of recent papers, the single-channel diffusion of different charged and uncharged particles through gramicidin A was treated both experimentally [6–10] and theoretically [10–16]. The

time dependence of the migration of the ions is commonly treated using a small set of kinetic equations for the particle hopping between different binding sites [12–14,22]. The number of sites and also the activation energies between them can be obtained either by fitting to the experimental transport rate [12–14] or using a variety of mean force models to obtain the potential energy as a function of the diffusing co-ordinate [18,22]. It has been demonstrated by Eisenman et al. [12,13] that the experimental results can be well interpreted by a four-site model, i.e., four potential minima along the channel direction separated by potential barriers. This model, however, gives no explanation of the microscopic origin of ion-specific properties. A better understanding of these effects can be expected if the microscopic structure of the gramicidin A molecule is taken into account and physically reasonable ion-channel interactions are considered in calculating static and dynamic properties of the ion-channel system. Some attempts toward a microscopic model based on rate theory were made by Läuger et al. [18,23], who studied a multi-site model which, in principle, takes into account the microscopic periodicity of the channel interior. The first more quantitative model was presented in the molecular dynamics study of Fischer et al. [24] who calculated ion-diffusion rates along the axis of a model channel consisting of a helical arrangement of polar carbonyl groups forming the hydrophilic pathway in gramicidin A. In that work [24], only pure electrostatic interactions between the ion and the flexible carbonyl groups were considered. It was demonstrated that the molecular dynamics results are qualitatively in agreement with those obtained from rate-theoretical predictions.

In their experimental work, Eisenman et al. [7,8] found that the single-channel conductance of the univalent cations Li^+, Na^+, K^+ and Rb^+ increases with increasing mass of the migrating particles; while absolute rate theory for site-to-site diffusion predicts a conductance inversely proportional to the square root of the mass of the ion [21,25]. In the present work, a theoretical mechanism is presented which relates the experimental inverse selectivity sequence ($Rb^+ > K^+ > Na^+ > Li^+$) [6–8] to the microscopic parameters of the channel-ion interaction. We use a molecular dynamics simulation technique to calculate the jump frequencies for the different cations in a model channel which is much more sophisticated than that presented earlier [24]. In this model, the ions are allowed to move not only along the channel axis but also perpendicular to it. In addition to the ionic potentials, van der Waals-type potentials for the ion-carbonyl interaction and repulsive non-ionic potentials were introduced. It will be demonstrated that the transition frequencies calculated in computer experiments have the correct experimental trend. The model approach will be described in section 2 while in section 3 some technical details are reviewed. Section 4 shows numerical results and in the last section some conclusions are drawn from our calculations.

2. Model approaches

2.1. Model of the channel

Molecular dynamics analysis of transport phenomena in the condensed phase is a very time-consuming procedure. The numerical effort drastically increases with the complexity of the model and the number of particles in the system. Therefore, in order to study the elementary microscopic steps of facilitated cation diffusion through ion translocators (channels) embedded in biomembranes, we used a simple model which mimics only the central hole of the helical transport molecule (see fig. 1). We have chosen model parameters closely related to the pore-forming dimer gramicidin A. This drastically reduces the number of free parameters because the structure and geometry of gramicidin A are well known [19,20]. In accordance with our earlier work [24] (in the following: paper I) we modelled the channel as a helical arrangement of dipolar ligands (carbonyl groups in gramicidin A). These ligands are represented by rigid dipoles. Their positive ends (carbon atoms) are fixed on a helix with six dipoles per single turn. The negative end of each dipole i (oxygen atom) can oscillate around an equilibrium angle φ_i^0 in a plane through the positive end of each dipole and the channel axis (see fig. 1). The undistorted motion of the

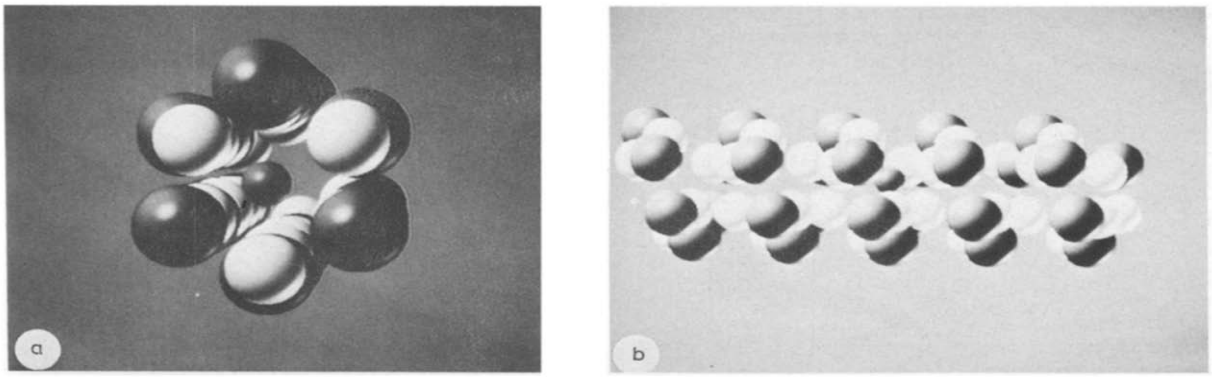

Fig. 1. Three-dimensional pictures of the model channel. (a) top view, (b) side view, generated by computer-aided design with the programme system MOLCAD of the authors institution.

dipole is a torsional harmonic vibration around φ_i^0 with frequency ν_t. The radius R of the helix is chosen so that the central hole of the pore is around 0.4 nm in diameter. The pitch h of the helix, the dipole length d, the alternating equilibrium arrangement of the dipoles and all other geometrical parameters of the model channel are chosen in imitation of the peptide gramicidin A (see table 2). The interaction between the ions and the channel dipoles is modelled by electrostatic and non-ionic contributions. The electrostatic interaction caused by the different partial charges is reduced to a sum of point charge interactions between the atoms of the dipolar ligands and the ion. The non-ionic interaction between the dipoles and the ion is modelled by the common Lennard-Jones (12,6) potential [26,27].

$$V(r) = 4\epsilon\left[(\sigma/r)^{12} - (\sigma/r)^{6}\right] \qquad (1)$$

This potential has only two parameters, the dissociation energy ϵ and the hardness parameter σ, which can be roughly identified with the radius of a sphere in the hard-sphere model. As described in a previous work [27] the specific parameters are obtained from standard values using combination rules. In contrast to the model presented in paper I [24], the ion is allowed to move not only along the channel axis but also perpendicular to it. In addition to the interactions described above, the motion of the ion is confined to the channel by introducing a repulsive interaction between the ion and the channel wall, which is described by the term $V_0(r'/r_0)^{12}$, where r' is the distance between the channel axis and the ion. This type of interaction takes into account the overlap of the electron distribution of the migrating particle and the peptide-forming atoms. The channel wall is simulated by an oxygen-like atom shell located around the helix with fixed radius R_W. The explicit parameters of this repulsive potential are drastically dependent on the size of the moving particle. The details of the calculation of V_0 and r_0 are given in appendix A.

The superposition of all interaction energies of the ion with its environment creates a potential energy $V(x, y, z)$ for the moving cation as a function of its migration co-ordinate z (channel axis) and the two perpendicular co-ordinates x and y.

It provides an energetically favourable pathway for the ion through the pore (in the rigid-pore approximation). The energy along this reaction path shows binding sites (potential minima) and energy barriers. Their depth and height are strongly correlated to the migrating ion species (see fig. 2).

The individual dipoles interact via electrostatic and Lennard-Jones-like interactions. This mutual coupling of the dipoles guarantees a fast energy transfer between them and thus a rather good thermalization of the dipoles. The channel acts as

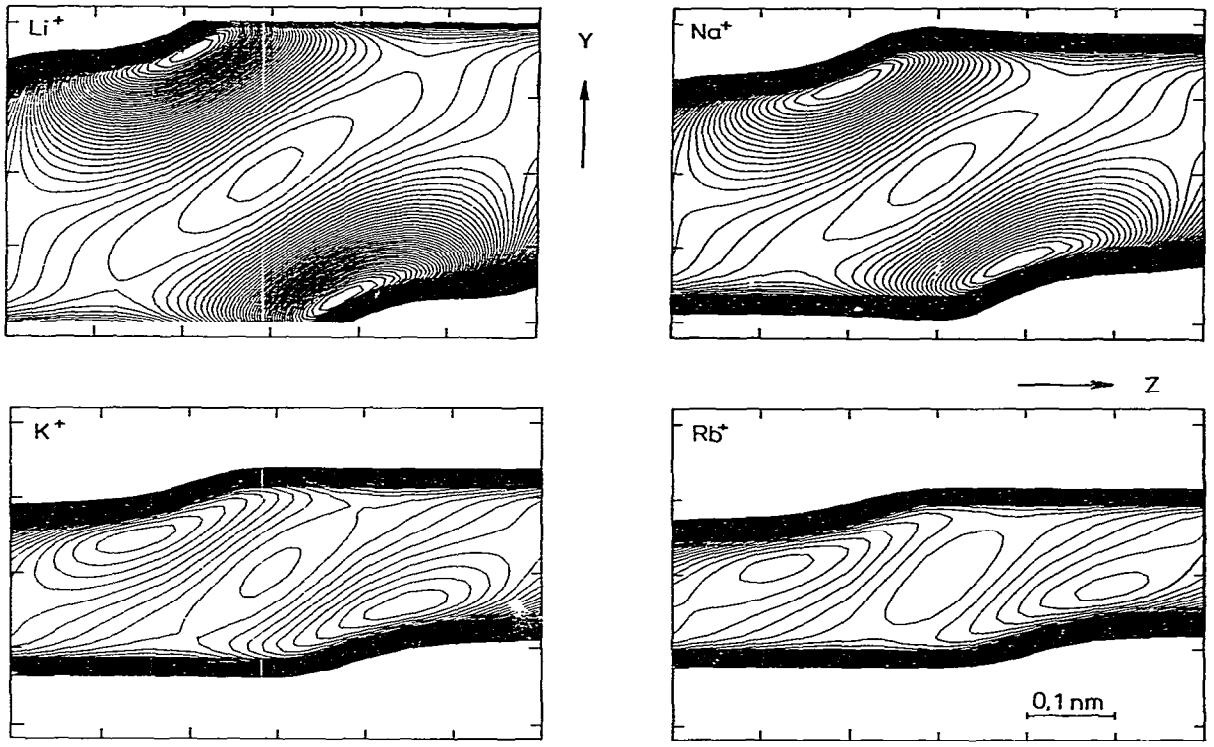

Fig. 2. Potential energy cuts for Li^+, Na^+, K^+ and Rb^+ along the channel axis. The flexible CO groups of the channel are held fixed in their equilibrium positions. The energy difference of two adjacent counter lines is $\Delta E = 0.01$ eV.

a thermal heat bath of definite temperature for the ion.

Our model approach, therefore, corresponds to the experimental situation inside those real channels (e.g., gramicidin A) in which the ion interacts with the ligand groups lining the central hole of the pore and the channel is thermalized by the membrane environment.

2.2. Molecular dynamics simulation techniques

The microscopic origin of selective particle transport in most biological systems is presently unknown. Kinetic equations on an empirical basis can only help to fit experimental results but cannot be used to study transport phenomena on a molecular level. This can be done if the macroscopic properties are derived from microscopic interactions and microscopic dynamics.

In the present work microscopic particle motions are calculated using a molecular dynamics technique recently applied to a variety of physical and chemical problems [28–30].

In this molecular dynamics scheme the classical equations of motion

$$\dot{q}_i = \mathrm{d}q_i/\mathrm{d}t = \partial H/\partial p_i, \quad \dot{p}_i = \mathrm{d}p_i/\mathrm{d}t = -\partial H/\partial q_i \qquad (2)$$

are solved simultaneously by numerical integration. Here (q_i, p_i) are the canonically conjugated position and momentum variables of the particles in the system, and $H = E_{kin} + V$ is the Hamiltonian for the total system (ion + channel) which

can easily be obtained from the microscopic description of the model (see appendix B). E_{kin} is the kinetic energy and V the potential energy.

The interesting dynamical variable is the ion-migration trajectory from which the macroscopic diffusion coefficient D can be easily calculated. We obtain this trajectory (position and momentum as a function of time) for the diffusing ion by numerically integrating eq. 2 for a given set of initial conditions. From the trajectory several dynamic properties, such as the site-to-site jump frequency k' of the ion and the temperature T of the system, can be determined.

We used periodic boundary conditions as in paper I to avoid artificial effects of the finite length of the channel. The average number of time steps per simulation is between 30000 and 75000 steps which corresponds to a system time period of about 100–250 ps

3. Calculation of the transition frequency k'

In a previous work [24] we tested the validity of rate-theory analysis as a description of ion transport in channels. This could easily be done, because the ion was constrained to move only along the channel axis. Therefore, a well defined reaction path for the ion was given and different potential energy curves could be calculated and studied relative to different sets of model data. In the model presented here the reaction path is not a priori well defined because the ion is allowed to move not only along the axis of the channel but also perpendicular to it.

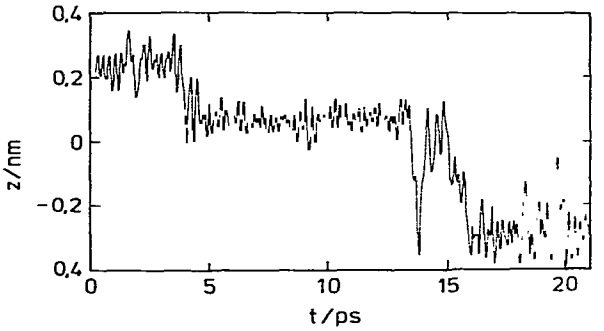

Fig. 3. Projection of a particular Na^+ trajectory in the model pore on the pore axis z as a function of time.

However, as one can seen from fig. 2, the ion potential inside the channel shows well defined quasi-equilibrium sites (potential minimum) and transition-state sites (saddle points). The ion carries out discrete jumps from one binding site into another as is demonstrated in fig. 3, where the z-co-ordinate of the ion trajectory is drawn as a function of time for a particular case. We can count the total number of jumps N_j of the ion from one site to a neighbouring one in a time period τ of the simulation and define the jump rate k' as

$$k' = N_j / 2\tau \tag{3}$$

k' is, therefore, the mean jump rate over one barrier in the forward or backward direction [18,24].

The diffusion coefficient D can be obtained from k' and the distance a of adjacent sites (jump length) as

$$D = a^2 k' \tag{4}$$

It is well known from experimental observations [31] that most hopping diffusion processes in ordered material show Arrhenius-type temperature behaviour. The diffusion coefficient can be formally given as

$$D = \nu_0(T) \exp[-E_a/kT] \tag{5}$$

where k is Boltzmann's constant and E_a the activation energy. The pre-exponential factor $\nu_0(T)$ is the average oscillation frequency of the ion in the quasi-equilibrium wells. It is weakly temperature dependent and inversely proportional to the square root of the particle mass m_1 if normal rate theory can be applied [18,23]

$$\nu_0(T) \propto m_1^{-1/2} \tag{6}$$

We used the variance of a binominal distribution [18,24] to estimate the statistical error involved in the numerical calculation of k'. This yields

$$\Delta N_j / N_j = \left(1 - N_j/(2\tau\nu_0)\right)^{1/2} N_j^{-1/2} \tag{7}$$

N_j is the total number of jumps during the simulation time τ. The oscillation frequency ν_0 can be

approximately obtained from the trajectory of the ion [24].

The temperature T of the system is calculated for every 500–1000 time steps of integration in the following manner:

$$T = \langle \frac{2}{k} \sum_{i=1}^{f} E_{kin}^{i} \rangle \qquad (8)$$

where f is the number of degrees of freedom and E_{kin}^{i} the kinetic energy per degree of freedom. The brackets indicate the time average. It is found that the calculated temperature T is constant in the range of $\pm 5\%$ during the simulation time.

4. Numerical results

As mentioned above, we used the molecular dynamics simulation method to calculate trajectories of the different univalent cations Li^+, Na^+, K^+ and Rb^+ in the model channel described in section 2.

In all calculations we used the Lennard-Jones (12.6) parameters and partial charges as given in table 1 [26]. The geometrical parameters of the present model channel are taken from the gramicidin A molecule [19,20]. They are listed in table 2.

Table 1

Interaction parameters for the different ions and the dipoles

	Lennard-Jones (12.6) parameters		Reference
	σ (m) ($\times 10^{-10}$)	ϵ (J) ($\times 10^{-23}$)	
Li^+-Li^+	2.75	0.58	26
Na^+-Na^+	2.94	8.10	
K^+-K^+	3.46	41.70	
Rb^+-Rb^+	3.62	78.40	
O-O	2.67	159.70	33, 34
C-C	3.76	132.00	
	Partial charges q		
Oxygen	$q_O = -0.38e_0$ [a]		35
Carbon	$q_C = 0.45e_0$		
Ions	$q_I = e_0$		

[a] Elementary charge $e_0 = 4.802 \times 10^{-10}$ e.s.u.

Table 2

Parameters used in the numerical calculations

Parameter		Reference
Helix radius, R	3.7×10^{-10} m	19, 20
Helix pitch, h	6.0×10^{-10} m	19, 20
Length of a unit cell	30.0×10^{-10} m	
C = O dipole length	1.24×10^{-10} m	35
Equilibrium angle, φ_i^0	$\pm 20°$	19, 20
Wave number, $\tilde{\nu}$	150–500 cm^{-1}	
Masses of particles		
Oxygen, m_O	2.655×10^{-26} kg	
Lithium, m_{Li^+}	1.152×10^{-26} kg	
Sodium, m_{Na^+}	3.817×10^{-26} kg	
Potassium, m_{K^+}	6.500×10^{-26} kg	
Rubidium, m_{Rb^+}	14.190×10^{-26} kg	
Time step, Δt	$0.2 - 0.6 \times 10^{-14}$ s	
Integration steps per run	30000–75000	

4.1. Temperature dependence of the transition frequency k'

Not all of our parameters can be directly related to real molecules, since they are not known from experiments. The most important one of this type is the force constant γ of the restoring force for the dipole vibration. In the undistorted case $\gamma \to 0$, the dipoles are freely rotating while for $\gamma \to \infty$, the dipoles become rigid. Consequently, the force constant can be viewed as a 'softness' parameter of the model channel and it is directly related to the nuclear polarizability of the helix. The force constant γ corresponds to the wave number $\tilde{\nu}$ of the dipole vibration (skeletal vibration)

$$\gamma = md^2\tilde{\nu}^2(2\pi c)^2 \qquad (9)$$

where m is the reduced mass of the oscillating dipole, d the dipole length and c the velocity of light. The range of possible wave numbers $\tilde{\nu}$ for the skeletal vibration is about 100–600 cm^{-1} which corresponds to a mean thermal amplitude $\Delta\varphi$ of the tilt angle of 10–2° at 300 K. This amplitude $\Delta\varphi$ can be evaluated as [18]

$$\Delta\varphi = \{\langle(\varphi_i - \varphi_i^0)^2\rangle\}^{1/2} = (kT/\gamma)^{1/2} \qquad (10)$$

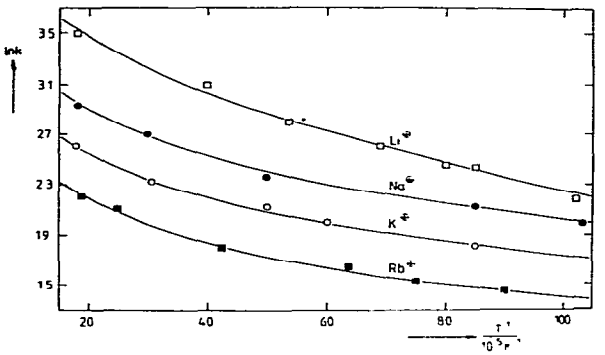

Fig. 4. Temperature dependence of relative jump rates k for Li^+, Na^+, K^+ and Rb^+ in the soft channel ($\tilde{\nu} = 150$ cm^{-1}) in the high-temperature range.

We first studied the temperature dependence of the ion-migration rate in the present model system. In a series of molecular dynamics simulations the transition rates k'_M were calculated for the different cations Li^+, Na^+, K^+ and Rb^+ by changing the total energy of the system. The temperature was determined according to eq. 8. The results of this simulation series in which the dipole oscillation frequency was fixed ($\tilde{\nu} = 150$ cm^{-1}) are shown in fig. 4. It can be seen from the Arrhenius plots in this figure that the calculated values of $\ln k'_M$ have approximately the same rate of decrease for all four cations Li^+, Na^+, K^+ and Rb^+.

We compare our results with those predicted from rate theory. According to eqs. 5 and 6 this theory [14,18,21] predicts that the shape of the Arrhenius plot is equal for all ions (temperature dependence) and that the transition rate k'_M is inversely proportional to the square root of the mass of the migrating ion M, i.e., $k'_M \propto (m_M)^{-1/2}$ (mass dependence). This mass dependence only causes a shift of the Arrhenius plot for the different ions but does not change the effective activation energy. Comparing the ratios of the transition frequencies k'_M/k'_{Na^+} calculated in our molecular dynamics simulations ($M = Li^+$, K^+, Rb^+) with the ratios of the masses $(m_M/m_{Na^+})^{-1/2}$ (table 3), it can be seen that our results reproduce the expected mass dependence of k'_M for different ions quite sufficiently. It is seen in fig. 4 that for temperatures less than 2500 K the values of $\ln k'_M$ fall roughly on parallel lines for the four cations while the higher temperatures ($T > 2500$ K) $\ln k'_M$ shows an unexpected increase. This is related to the fact that the pre-exponential factor ν_0 in eq. 5 dominates the temperature dependence of the rate constant. The latter result could also be verified in a more sophisticated rate-theoretical analysis of

Table 3

Comparison of the ratios of the site-to-site jump rates k'_M/k'_{Na^+} for $M = Li^+$, K^+ and Rb^+

M	M/Na^+ (from ref. 8)	$(m_M/m_{Na^+})^{-1/2}$	k'_M/k'_{Na^+} (from this work)				
			a	b	c	d	e
Li^+	0.32 0.32 0.24	1.82	1.79	1.37	0.50	0.30	0.58
K^+	2.33 2.01 1.93	0.77	0.72	0.74	1.76	2.20	1.32
Rb^+	3.08 2.88 3.17	0.52	0.50	0.53	1.33	2.67	1.50

[a] From molecular dynamics simulation for the soft channel ($\tilde{\nu} = 150$ cm^{-1}, $T \approx 5000$ K).
[b] From molecular dynamics simulation for the soft channel ($\tilde{\nu} = 150$ cm^{-1}, $T \approx 1200$ K).
[c] From molecular dynamics simulation for the rigid channel ($\tilde{\nu} = 150$ cm^{-1}, $T \approx 1200$ K).
[d] Like [c] but for equal masses of the migrating ion ($m_M = m_{Na^+}$).
[e] From molecular dynamics simulation for the rigid channel with large radius ($\tilde{\nu} = 500$ cm^{-1}, $T = 1200$ K, $R = 0.7$ nm).

our model [22]. We, therefore, conclude that the transition frequencies k'_M calculated in our molecular dynamics simulations in the case discussed above ($\tilde{\nu} = 150$ cm^{-1}) show just the mass and temperature dependence as expected from common rate theory.

As has been pointed out, the molecular dynamics simulation technique is a very-time consuming computer procedure. In our calculations a time interval of 100 ps corresponds to a run time of around 10–30 h (CPU time on a PDP 11/60) depending on the highest forthcoming frequency in the simulated system. This basic oscillation frequency is approx. 10^3-times larger than the jump rate k'_M for total energies of the system which correspond to kT at room temperature, i.e., there is only one site-to-site jump within a period of 1000 oscillations of the ion. Consequently, it takes an enormously long time to perform a calculation series with a sufficient number of transitions under these conditions. We, therefore, increased the total energy up to values corresponding to temperatures larger than 800 K to obtain at least one jump per 200 oscillations.

The temperature dependence of the jump frequency k'_M discussed above (see fig. 4) indicates (in accordance with paper I) that our results can be well extrapolated down to room temperature.

4.2. Influence of the skeletal vibration on the specificity of the channel

In our numerical treatments with $\tilde{\nu} = 150$ cm^{-1}, we found a selectivity sequence Li > Na > K > Rb which corresponds to the Eisenman sequence XI [36,37]. However this sequence is not found in the gramicidin A dimer. Experimental investigations [6–8] show that the single-channel conductivity of gramicidin A for the univalent cations Li^+, Na^+, K^+ and Rb^+ increases with increasing mass of the diffusing ion (see table 3). This corresponds to a selectivity sequence of Rb > K > Na > Li which is the inverse of that given above.

In order to find out which microscopic parameters of a channel may cause this inverse ion specificity (Eisenman sequence I) we first investigate the influence of the wave number $\tilde{\nu}$ of the torsional vibration of the dipolar ligands on the migration rate. This softness parameter is the only freely selectable parameter of our model channel. We carried out a series of computer experiments to calculate the transition frequency k'_M for each univalent cation ($M = Li^+$, Na^+, K^+, Rb^+) in which the wave number of the C = O torsional vibration was chosen to be 150, 270, 330 and 500 cm^{-1}. The continuous variation of only one model parameter (with all others held fixed during a 'numerical experiment') enables us to study the influence of each model parameter independently. This is the great advantage of this method in comparison to real experiments. During the calculations described here a temperature $T = 1200$ K was chosen. The geometrical parameters of the channel are the same as given in table 2. The results of the simulation series are shown in fig. 5. It is seen that the jump frequencies k'_M for the different ions are non-monotonous functions of the dipole oscillation frequencies. The transition frequencies k'_M of the lighter ions Li^+ and Na^+ strongly decrease with increasing wave number $\tilde{\nu}$ while the rates of K^+ and Rb^+ are roughly independent of the softness of the C=O dipole vibration. In rate-theoretical analysis, Läuger [18] also produced non-monotonous specificity sequences.

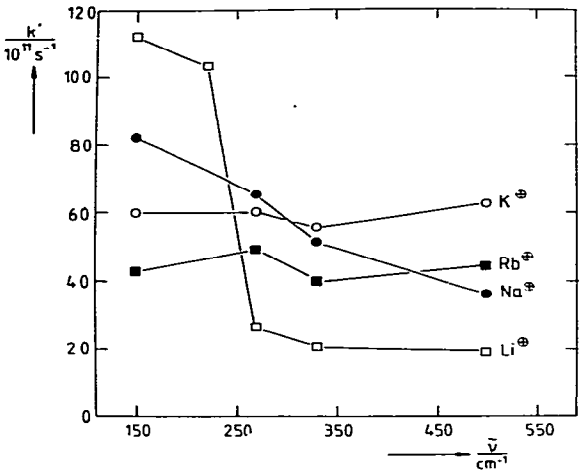

Fig. 5. Site-to-site transition rates k' for different alkali metal cations as functions of the softness of the channel (represented by the CO-bonding mode $\tilde{\nu}$).

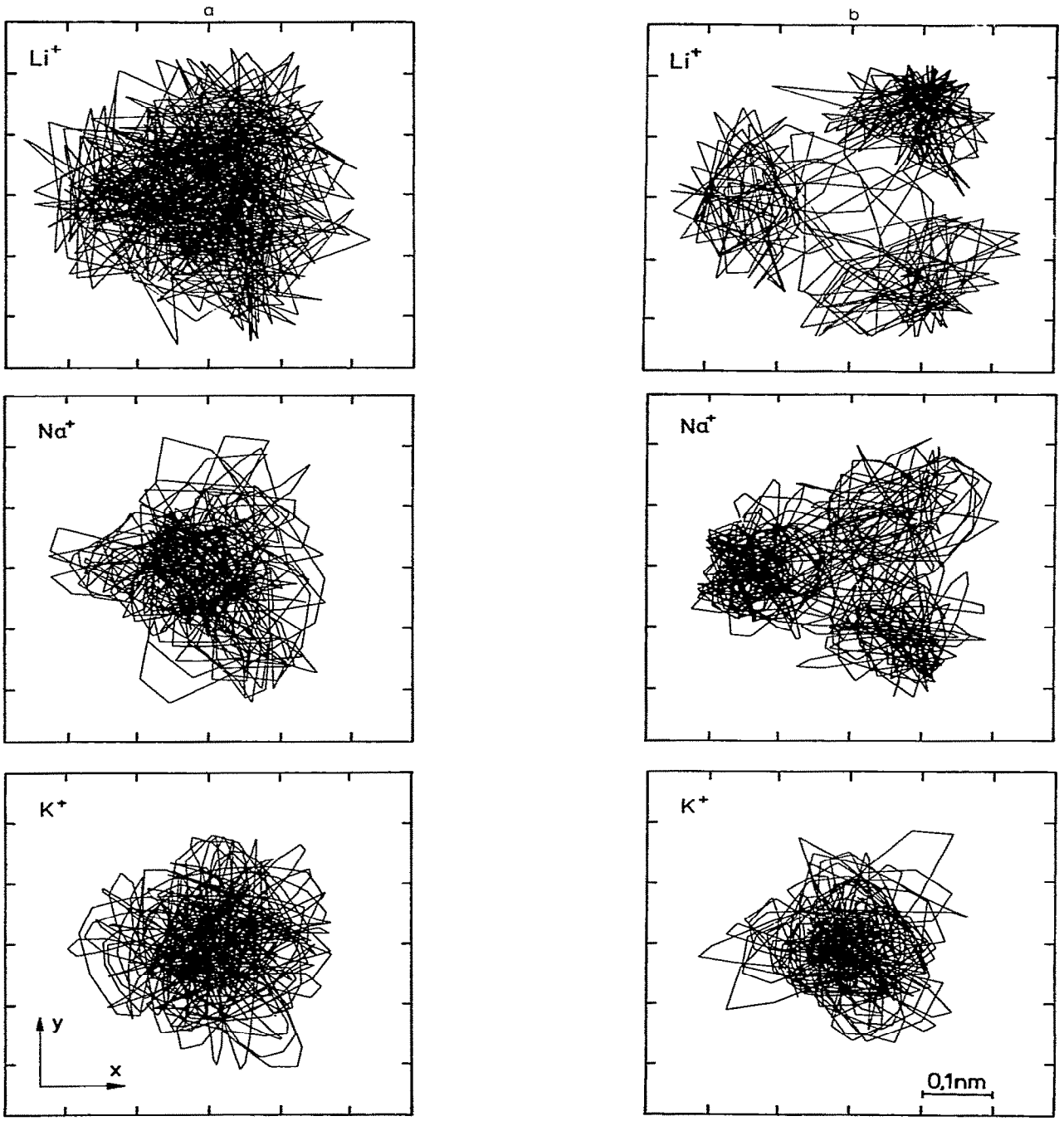

Fig. 6. Projection of different ion trajectories on the x-y plane (perpendicular to the channel axis) in a soft channel (a) with $\tilde{\nu} = 150$ cm^{-1} and a rigid channel (b) with $\tilde{\nu} = 500$ cm^{-1}.

but he found the inverse tendency relative to our results. This may be an effect of the special parameters that Läuger [18] used. The ratios of the jump rates k'_M/k'_{Na} (M = Li^+, K^+ or Rb^+) for a wave number of $\tilde{\nu} = 500$ cm^{-1} are listed in table 3. These ratios correspond to a selectivity sequence of K > Rb > Na > Li (Eisenman sequence II a). This means that for the hard channel ($\tilde{\nu} = 500$ cm^{-1}) our calculated ratios show just the trend found experimentally [6,8].

The different specificity sequences for different flexibility of the ligand system results from combined effects of the coulomb interaction, which is identical for all ions, and the ion-specific Lennard-Jones interactions between the ions and the ligand system. The transition frequency depends not only on the mass of an ion and the energy barrier separating two wells, but also very sensitively on the sizes of the migrating particles. The latter effect can be related to entropy phenomena. It was shown in a recent work by the present authors [27] that this entropy effect causes an increase in the transition frequency for increasing size of the ion in narrow ion channels. It was demonstrated therein that the size effect outweighs the normal mass dependency of the diffusion rate, i.e., larger and heavier ion may migrate faster through transmembrane channels than smaller and lighter ones. This relation of the transition rate to the ion size is much more pronounced for the rigid channel ($\tilde{\nu} = 500$ cm^{-1}) than for the soft channel ($\tilde{\nu} = 150$ cm^{-1}). In fig. 6a and b the projections of the ion trajectories on the x-y plane (perpendicular to the channel axis) for the four cations Li^+, Na^+, K^+ and Rb^+ are drawn. Fig. 6a shows the trajectories in the soft channel ($\tilde{\nu} = 150$ cm^{-1}) and fig. 6b those in the rigid channel ($\tilde{\nu} = 500$ cm^{-1}). It is seen that the ions migrate in a qualitatively different manner through the soft and rigid channels. In the soft channel all ions migrate around the channel axis roughly in the same manner, i.e., the size effect can be neglected and only the mass effect determines the selectivity sequence (see table 3). In a more rigid channel (fig. 6b), we observe three quasi-equilibrium sites per helix turn, each displaced from the channel axis. This pattern becomes more pronounced for the smaller ions. In the latter case the mass effect is outweighed by the size effect (see fig. 5) and the selectivity sequence depends strongly on both the mass and the size of the ion. To study only the size effect in the rigid channel we performed also a simulation series wherein all migrating particles have the same mass but different size. We calculated the transition frequencies of univalent ions with the mass of Na^+ but with different sizes (Lennard-Jones parameters as given in table 1). No mass effects are possible in this simulation series; all differences in the results are only consequences of the size of the particles, i.e., the different non-ionic interactions between the ion and the channel particles. The ratios of k'_M/k'_{Na} found in this numerical simulation are 0.30, 2.24 and 2.72 where the interaction parameters for Li^+, K^+ and Rb^+, respectively, were used for M. Comparing these ratios with the experimental [6–8] ratios of 0.29, 2.20 and 3.04 (mean values), we find that the ion specificity sequence Rb > K > Na > Li is just that found for gramicidin A. Moreover, the values of the ratios are in very good agreement with experiment. This result agrees with the experimental evidence that ions in channels like the gramicidin A system probably should be considered not as isolated particles but as partly solvated complexes [5,10,11]. Water molecules are simultaneously transported. This fact may lead to effective masses of the migrating particle which are larger than those of the ions and which approach each other if the number of solvent molecules is the same for all ions.

5. Potential energy cuts

In the molecular dynamics simulations presented in this article the migrating particles are not constrained to move along the channel axis (x-axis). The three-dimensional reaction path for the moving ions (way of steepest descent in the potential energy surface) is not known a priori. This lack of information can partly be overcome by calculating series of potential cuts along the axis of the channel and perpendicular to it where the channel particles are fixed. In fig. 2 the contour maps of the two-dimensional potential function $V(y, z)$ are plotted for the univalent cations Li^+,

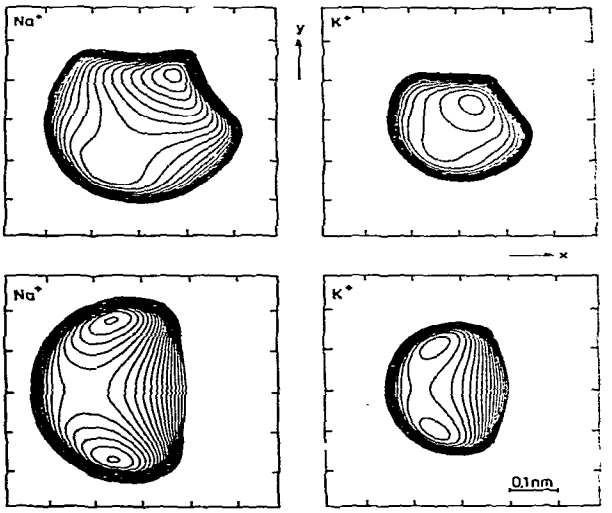

Fig. 7. Potential energy cuts for Na^+ (a) and K^+ (b) perpendicular to the channel axis for the quasi-equilibrium sites (upper figures) and the transition states (lower figures).

Na^+, K^+ and Rb^+ with $V(y, z)$ giving the potential energy (see appendix) of an ion at the position $(0, y, z)$. The dipoles are fixed to their equilibrium position which is roughly φ_i^0. Potential cuts perpendicular to the channel axis (x-y plate) are given in fig. 7 for the two ions Na^+ and Rb^+. The z value is varied between two quasi-equilibrium sites. The pitch of the helix in the calculation of the two-dimensional energy functions was chosen to be 1.2 nm in order to get a better resolution in the contour maps. It can be seen from fig. 2a–d that the potential energy along the z-axis ($x = y = 0$) has nearly the same curvature for all four cations. This fact indicates that the potential along the center of the channel is mainly determined by coulomb forces. Away from the channel axis, the potential energy function changes very drastically with the type of cation. The available 'space' (in the x-y plane) of the migrating particle increases with decreasing size of the particle (see figs. 2 and 7). As we have shown in a recent paper on ion transport in narrow systems [27], these differences in the free 'volume' for the motion of each ion contribute to the activation entropy. The latter strongly influences the frequency k' of penetration of the potential barrier separating two quasi-equilibrium sites. We also showed that the transition frequency increases if the free volume at the quasi-equilibrium site decreases. Consequently, we expect an increasing jump rate with increasing size of the migrating particle. However, the size of the ion does not only effect the activation entropy as can be seen from fig. 2. The potential minima become deeper for the smaller ions. This additional size effect may also contribute to the transition frequency in an inverse way to the selectivity sequence predicted from only the mass of the migrating particle. Both size effects are determined mainly by the short-range (repulsive) part of the Lennard-Jones interaction and the coulombic interaction between the ion and the carbonyl groups (see table 1). It is now obvious that an $m^{-1/2}$ dependency of the ion transition rate may occur in the soft channel ($\bar{\nu} \approx 150\ cm^{-1}$) and that the situation changes for more rigid pores. The reason is that the relatively large thermal amplitude of the dipole vibrations in the soft channel (≈ 10–$15°$) effaces the size-selective inner structure of the channel for the different cations and the only selective effect is the mass effect. The situation changes if the channel becomes more rigid and the size-selective character of the binding sites becomes more pronounced and the size effect partly outweighs the mass effect, causing a change in the selectivity sequence, as indicated in fig. 5.

To improve the understanding of the specificity of the channel a series of computer experiments for the rigid channel was performed in which the radius R of the pore is enlarged to around 0.55 nm. The masses of the migrating particles are taken as that of Na^+ (all other parameters are the same as given in table 2) so that no mass effect is expected. For such a large channel radius the 'free volume' is nearly the same for all four univalent cations and consequently no entropy effects are expected either (as has been shown by the authors [27]). In this case we found that the absolute transition frequency is roughly twice that in a narrow channel ($R \approx 0.2$ nm) and the ratios of the rates k'_M/k_{Na^+} with interaction parameters from Li^+, K^+ and Rb^+ are 0.58, 1.32 and 1.50, respectively. These ratios are roughly the same as that

found for single-ion conductance in aqueous solution (0.7, 1.5 and 1.6) where also no mass effect is expected [6]. The differences in the jump frequencies are now only caused by the different depths of the potential minima at the binding sites. The latter are strongly influenced by the local interaction between the ion and the carbonyl groups.

6. Conclusions

In the present work the influence of microscopic parameters, such as atomic coordinates and force constants, on the transition frequencies of different alkali metal cations in a transmembrane model channel was investigated by means of the molecular dynamics technique. The structure and the dynamics of the channel were modelled as a set of interacting CO groups located on a hexagonal helix chain of which the microscopic parameters are roughly those of the gramicidin A polypeptide channel. The transition frequencies for the four cations Li^+, Na^+, K^+ and Rb^+ were calculated from the trajectories (which result from the molecular dynamics computer experiments) as a mean site-to-site jump rate, from which the overall permeability (and conductance) of the channel can be obtained in a straightforward manner [14,21,25].

A parameter which is of central importance for the specificity of the channel is the vibrational frequency of the hydrophilic CO groups which can be viewed as the 'softness' of the skeletal vibration of the channel. It was shown that this softness parameter strongly influences the selectivity sequence of the channel. This ability to discriminate between different ions results from the combined effects of the mass and the size of the ion. The main results can be summarized as follows:

(i) The transition frequency increases with decreasing ratio of the channel radius to the ion radius (entropy effect). This effect becomes much more pronounced in narrow channels ($R = 0.2$–0.4 nm) than in larger ones.

(ii) The potential minima at the quasi-equilibrium sites become much deeper for the smaller ions than for the larger ones while the potential energy at the transition point is roughly the same for all ions. This depth, which is nearly independent of the channel radius, causes an increase in the activation energy with decreasing size of the migrating particle.

(iii) The former two size effects are inverse to the $m^{-1/2}$ dependence of the transition frequency (m, mass of ion) and obviously outweigh the mass effect.

(iv) Therefore, the selectivity sequence of a channel depends very sensitively on the balance of the size and mass effects.

(v) The softness of the channel determines how much the size effect becomes pronounced. This means that the softness strongly influences the specificity of the pore.

It is seen that the molecular dynamics simulation technique is well suited to the study of the microscopic steps of ion transport through model channels, at least for qualitative predictions. It should be stressed that the overall permeability of a channel not only depends on the site-to-site transition frequency but also on the rate of association (dehydration) of the ion with the channel and on the dissociation (hydration) of the ion to the liquid [12,13] and also on the presence of other transported particles in the channel (for example water molecules). The dependence on these parameters is the subject of further investigation.

Appendix A

A.1. The potential energy $V(r) = V_0(r/r_0)^{12}$

We introduce a repulsive interaction for the ion perpendicular to the channel axis in the following manner:

$$V(r') = V_0(r'/r_0)$$

where r' is the distance of the ion from the z-axis ($r' = (x^2 + y^2)^{1/2}$), V_0 is chosen as 5×10^{-21} J and r_0 is an ion-specific repulsive radius. The latter parameter r_0 is calculated so that the repulsive continuum is equal, i.e., of the same matter, for every cation. For a given radius R_W (see fig. 8) we define r_0 as

$$r_0 = R_W - r_I$$

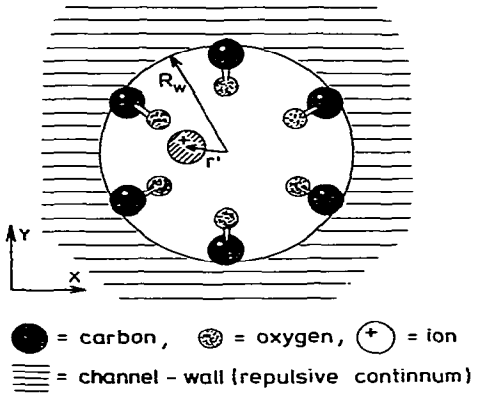

Fig. 8. Arrangement of the carbonyl groups in the model pore (schematically).

where $r_I (I = Li^+, Na^+, K^+, Rb^+)$ can be calculated from the following equation (see fig. 9):

$$V(R_w - \sigma_{Iw}) = V_0 \left(\frac{R_w - \sigma_{Iw}}{R_w - r_I} \right)^{12} = \epsilon_{Iw}$$

where σ_{Iw} and ϵ_{Iw} are the Lennard-Jones (12,6) parameters of the ion-oxygen interaction calculated with the Lorenz-Berthelot rules [26,32]

$$\sigma_{Iw} = (\sigma_{OO} + \sigma_{II})/2$$

$$\epsilon_{Iw} = (\epsilon_{OO}\epsilon_{II})^{1/2}$$

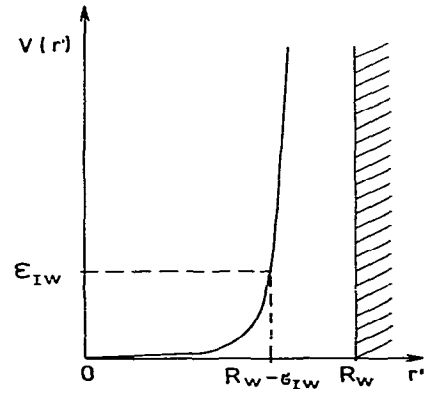

Fig. 9. Repulsive ion-channel wall potential as a function of the distance r' from the channel axis.

from the Lennard-Jones (12,6) parameters $(\sigma_{OO}, \epsilon_{OO})$ and $(\sigma_{II}, \sigma_{II})$ given in table 1.

Appendix B

B.1. The Hamiltonian $H = K_{kin} + V$

We assume in our numerical calculations that the interaction between the particles can be described via two-body interactions which are composed of Lennard-Jones and coulombic interactions. In addition to these two-body contributions, the potential energy V of the ion-ligand system contains energy terms from the harmonic restoring forces which depend on the tilt angle φ_i of the dipoles (fig. 10) and from the repulsive interaction of the ion with the channel wall, described in appendix A.

To calculate the Lennard-Jones parameters σ_{ij} and ϵ_{ij} for two different species we apply the common combination rules of Lorenz-Berthelot [26,32], $\epsilon_{ij} = (\epsilon_{ii}\epsilon_{jj})^{1/2}$ and $\sigma_{ij} = (\sigma_{ii} + \sigma_{jj})/2$. Using the co-ordinates R_1^i, R_2^i, r_1^i and r_2^i as given in fig. 10 and the ϵ_{ii} and σ_{ii} as listed in table 1, the potential energy V is then obtained as:

$$V = V(\varphi_1, \ldots, \varphi_N, x, y, z)$$

where

$$V = \frac{1}{2} \sum_{i=1}^{N} \gamma (\varphi_i - \varphi_i^0)^2 + V_0 \left[\frac{(x^2 + y^2)^{1/2}}{r_0} \right]^{12} + \sum_{i=1}^{N} \sum_{j<i} \left(\frac{q_0^2}{R_1^{ij}} + \frac{q_0 q_C}{R_2^{ij}} + \frac{q_0 q_C}{R_2^{ij}} \right)$$

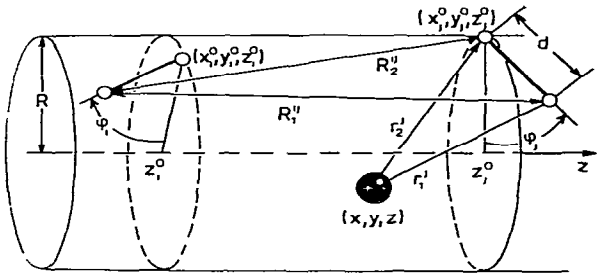

Fig. 10. Co-ordinates describing the interactions between the migrating cations at position (x, y, z) and dipoles i and j.

$$+\sum_{i=1}^{N}\sum_{j<i}4\epsilon_{OO}\left[\left(\frac{\sigma_{OO}}{R_4^{ij}}\right)^{12}-\left(\frac{\sigma_{OO}}{R_2^{ij}}\right)^{6}\right]$$

$$+\sum_{i=1}^{N}\sum_{j<1}4\epsilon_{CO}\left[\left(\frac{\sigma_{CO}}{R_4^{ij}}\right)^{12}+\left(\frac{\sigma_{CO}}{R_2^{ij}}\right)^{12}-\left(\frac{\sigma_{CO}}{R_2^{ij}}\right)^{6}-\left(\frac{\sigma_{CO}}{R_2^{ij}}\right)^{6}\right.$$

$$+\sum_{i=1}^{N}4\epsilon_{IO}\left[\left(\frac{\sigma_{IO}}{r_1^i}\right)^{12}-\left(\frac{\sigma_{IO}}{r_1^i}\right)^{6}\right]$$

$$+\sum_{i=1}^{N}4\epsilon_{IC}\left[\left(\frac{\sigma_{IC}}{r_2^i}\right)^{12}-\left(\frac{\sigma_{IC}}{r_2^i}\right)^{6}\right]$$

$$+\sum_{i=1}^{N}\left(\frac{q_I q_O}{r_2^i}+\frac{q_I q_C}{r_2^i}\right)$$

The kinetic energy is easily obtained as:

$$E_{kin}=\frac{1}{2}\sum_{i=1}^{N}m_O d^2\dot{\varphi}_i^2+\tfrac{1}{2}m_I(\dot{x}^2+\dot{y}^2+\dot{z}^2).$$

The coordinates R_1^{ij}, R_2^{ij}, r_1^i and r_2^i depend on the position and angle variables in the following manner:

$$R_1^{ij}=R_1^{ij}(\varphi_i,\varphi_j,x_i^0,y_i^0,z_i^0,x_j^0,y_j^0,z_j^0)$$

$$R_2^{ij}=R_2^{ij}(\varphi_i,x_i^0,y_i^0,z_i^0,x_j^0,y_j^0,z_j^0)$$

$$r_1^i=r_1^i(x,y,z,\varphi_i,x_i^0,y_i^0,z_i^0)$$

$$r_2^i=r_2^i(x,y,z,x_i^0,y_i^0,z_i^0)$$

Acknowledgements

We like to thank Professor Peter Läuger and Dr. Harald Schröder, both Konstantz, and Professor George Eisenman, Los Angeles, for critical comments. We are also indebted to Dr. E.E. Polymeropoulos and Dr. R. Pfeiffer for proof-reading the manuscript. This research was supported by the Deutsche Forschungsgemeinschaft, Bonn, and the Fonds der Chemischen Industrie, Frankfurt. This work is a part of the Ph.D. dissertation of W.F.

References

1 S.J. Singer, Annu. Rev. Biochem. 43 (1974) 805.
2 A. Rothstein, Z.I. Cabantchik and P. Knauf, Fed. Proc. 35 (1976) 3.
3 O.S. Andersen and J. Procopio, Acta Physiol. Scand. Suppl. 481 (1980) 481.
4 P. Läuger, J. Membrane Biol. 57 (1980) 163.
5 A. Finkelstein and O.S. Andersen, J. Membrane Biol. 59 (1981) 155.
6 S.B. Hladky and D.A. Haydon, Biochim. Biophys. Acta 274 (1972) 294.
7 G. Eisenman, J. Sandblom and E. Neher, Biophys. J. 22 (1978) 307.
8 E. Neher, J. Sandblom and G. Eisenman, J. Membrane Biol. 40 (1978) 97.
9 P. Läuger, R. Benz, G. Stark, E. Bamberg, P.C. Jordan, A. Fahr and W. brock, Q. Rev. Biophys. 14 (1981) 513.
10 J.A. Dani and D.G. Levitt, Biophys. J. 35 (1981) 485.
11 J.A. Dani and D.G. Levitt, Biophys. J. 35 (1981) 501.
12 G. Eisenman, J. Sandblom and J. Hagglund, in: Structure and function in excitable cells, eds. W. Adelman, D. Chang, R. Leuchtag and I. Tasaki (Plenum, New York, 1983) in the press.
13 G. Eisenman and J.P. Sandblom, in: Physical chemistry of transmembrane ion motions, ed. G. Spach, Proceedings of 36th International Conference of Société de Chimie Physique (Elsevier, Paris, 1983) p. 329.
14 P. Läuger, Biochim. Biophys. Acta 311 (1973) 423.
15 B. Hille, in: Membranes, a series of advances, vol. 3, ed. G. Eisenman, (Marcel Dekker, New York, 1975).
16 B.W. Urban and S.B. Hladky, Biochim. Biophys. Acta 554 (1979) 410.
17 J. Sandblom, G. Eisenman and J.V. Hagglund, J. Membrane Biol. (1982) in the press.
18 P. Läuger, Biophys. Chem. 15 (1982) 89.
19 D.W. Urry, Proc. Natl. Acad. Sci. U.S.A. 68 (1971) 672.
20 D.W. Urry, M.C. Goodall, J.D. Glickson and D.F. Mayers, Proc. Natl. Acad. Sci. U.S.A. 68 (1971) 1907.
21 B.J. Zwolinsky, H. Eyring and C.E. Reese, J. Phys. Chem. 53 (1949) 1426.
22 H. Schröder, J. Chem. Phys. 79 (1983) 1997.
23 P. Läuger, W. Stephan and E. Frehland, Biochim. Biophys. Acta 602 (1980) 167.
24 W. Fischer, J. Brickmann and P. Läuger, Biophys. Chem. 13 (1981) 105.
25 T.L. Hill, Statistical thermodynamics (Addison-Wesley, Reading, 1960).
26 W. Fischer and J. Brickmann, Ber. Bunsenges. Phys. Chem. 86 (1982) 650.
27 J. Brickmann and W. Fischer, Biophys. Chem. 17 (1983) 245.
28 P. Lykos, Computer modelling of matter, ACS Symposium Series 86 (1978).
29 E.E. Polymeropoulos and J. Brickmann, Chem. Phys. Lett. 92 (1982) 59.
30 W.F. van Gunsteren and M. Karplus, Biochemistry 21 (1982) 2259.
31 G. Alefeld and J. Völkl, Topics in applied physics, vols. 28+29 (Springer, Berlin, 1978).
32 D. Henderson, Annu. Rev. Phys. Chem. 25 (1974) 461.
33 S. Lifson and A. Warshel, J. Chem. Phys. 49 (1968) 5116.

34 A. Warshel, M. Levitt and S. Lifson, J. Mol. Spectrosc. 33 (1970) 84.
35 G.E. Schulz and R.H. Schirmer, Principles of protein structure (Springer, New York, 1979).
36 G. Eisenman, in: Ion selective electrodes, ed. R.A. Durst (National Bureau of Standards Special Publication 314, U.S. Government Printing Office, Washington, 1969) p. 1.
37 S. Krasne, in: Membrane physiology, eds. T.E. Andreoli, J.F. Hoffman and D.D. Fanestil (Plenum, New York, 1980) p. 217.